Journal of Physiology (1993), **468**, *pp.* 441–461
With 10 figures
Printed in Great Britain

ANOMALOUS PERMEATION OF Na^+ THROUGH A PUTATIVE K^+ CHANNEL IN RAT SUPERIOR CERVICAL GANGLION NEURONES

BY YU ZHU AND STEPHEN R. IKEDA

From the Department of Pharmacology and Toxicology, Medical College of Georgia, Augusta, GA 30912-2300, USA

(*Received 17 September 1992*)

SUMMARY

1. An unanticipated inward tail current was recorded from freshly isolated adult rat superior cervical ganglion (SCG) neurones using the whole-cell variant of the patch-clamp technique. The tail current was present when Na^+ was substituted for tetraethylammonium (TEA) as the primary monovalent cation in external solutions designed to isolate Ca^{2+} channel currents (0·5 μM tetrodotoxin present and K^+ omitted).

2. The tail current was observed following step potentials positive to −30 mV and reached half-activation near −9·0 mV. The decay of the tail current was voltage dependent and could be described with two time constants. Between potentials of −120 and −70 mV, τ_f, the fast component, varied from 3 to 8 ms and τ_s, the slow component, changed from 12 to 30 ms, respectively.

3. The tail current was not carried by Ca^{2+}, and did not appear to flow through a voltage-gated Ca^{2+} channel or a Ca^{2+}-dependent channel as it persisted in the absence of external Ca^{2+} or in the presence of the Ca^{2+} channel blocker, Cd^{2+} (0·1 mM).

4. Varying the external $[Cl^-]$ did not alter the reversal potential of the tail current indicating that Cl^- was not the charge carrier.

5. The reversal potential of the tail current changed in accordance with the Nernst relationship when $[Na^+]_i/[Na^+]_o$ was altered. Our results suggested that this 'unusual or unanticipated current' (I_u) was carried primarily by Na^+.

6. I_u was inhibited by the K^+ channel-blocking agents quinidine (0·1 mM), external Ba^{2+} (5 mM) and internal Cs^+ (145 mM). TEA (20 mM either internally or externally) and dendrotoxin (10 μM) were not effective inhibitors of I_u.

7. The decay time constants of the tail current and parameters of activation and inactivation of I_u were similar to those of TEA-insensitive delayed rectifier-type K^+ channel currents observed in the presence of 145 mM external K^+.

8. I_u was reduced in the presence of either external or internal K^+. The interaction of external K^+ with Na^+ on the I_u tail amplitude was reminiscent of anomalous mole-fraction behaviour.

9. Ion permeability studies revealed that the channel producing I_u had a permeability sequence to monovalent cations of 3·5:2·5:2:1:0·5 for Rb^+, K^+, Cs^+, Na^+ and Li^+, respectively.

10. These data suggest that in the absence of external K^+, the ion selectivity of a

TEA-insensitive K^+ channel in sympathetic neurones is profoundly diminished. Under these conditions, Na^+ traversing a K^+ channel can generate an unanticipated inward current. Therefore, caution should be observed in the interpretation of inward Ca^{2+} currents when recorded in the presence of external Na^+.

INTRODUCTION

To understand the function of voltage-gated ion channels better, it is often necessary to dissect the total whole-cell current into discrete current components carried by a single ion species. A commonly used strategy to isolate an individual current component involves the substitution of unwanted ions with non-permeant ions and/or blocking unwanted ion channels with pharmacological agents. For example, to isolate the Ca^{2+} channel current in rat sympathetic neurones from other voltage-activated currents, we commonly substitute the non-permeant cation *N*-methyl-D-glucamine (NMG) for internal K^+, substitute tetraethyl-ammonium (TEA) for external Na^+ (which also serves to block some K^+ channels) and add tetrodotoxin (TTX) to block the voltage-gated Na^+ channels. This combination of agents has been used successfully to study various aspects of neurotransmitter modulation of Ca^{2+} currents in freshly dispersed single neurones from adult rat superior cervical ganglion (SCG) (Ikeda, 1991, 1992). A drawback of this approach, however, is that TEA (especially at concentrations > 10 mM) has been reported to block muscarinic acetylcholine receptors in neurones (Brown & Constanti, 1980) and to reduce the muscarinic receptor-mediated inhibition of the Ca^{2+} currents in neuroblastoma–glioma hybrid cells (Caulfield, 1991). Moreover, the effects of TEA on the concentration–response curves for muscarinic agents appear to be different for agonist and antagonists thereby obfuscating the interpretation of pharmacological studies (Caulfield, 1991). Thus, in an attempt to avoid the undesirable effects of TEA on muscarinic acetylcholine and possibly other neurotransmitter receptors, we recorded Ca^{2+} currents in rat sympathetic neurones using an external solution containing Na^+ (and TTX), rather than TEA, as the major external cation. As previous studies (Schofield & Ikeda, 1988) have demonstrated that voltage-gated Na^+ channels in sympathetic neurones are completely blocked by TTX, we did not anticipate that this alteration would significantly affect our ability to isolate Ca^{2+} channel currents. Unexpectedly, however, under these conditions an unusually large and slow tail current appeared (see Fig. 1) which did not appear to be consistent with Ca^{2+} channel deactivation. The purpose of this study was to identify the ionic basis and possible channel(s) involved in producing this unusual tail current and to examine the practical and theoretical significance of this phenomenon.

METHODS

Isolation of single neurones

The method used to isolate single neurones from adult rat SCG has been described previously (Ikeda, 1991, 1992). Briefly, male Wistar rats (12–14 weeks old) were decapitated using a laboratory guillotine without prior anaesthesia and SCG dissected in cold Hanks' balanced salt solution. The ganglia were desheathed, cut into small pieces and then incubated with 1·2 mg ml^{-1} collagenase type D, 0·4 mg/ml trypsin (both from Boehringer Mannheim Biochemicals,

Indianapolis, IN, USA), and 0·1 mg/ml DNase type I (Sigma Chemical Co., St Louis, MO, USA) in 10 ml of Earle's balanced salt solution at 35 °C for 1 h in a shaking water bath. After incubation, cells were dissociated by vigorous shaking of the flask. After centrifugation at 50 *g*, the dispersed neurones were resuspended in minimum essential medium containing 10% fetal calf serum, 1% glutamine and 1% penicillin–streptomycin solution (all from Gibco, Grand Island, NY, USA). Neurones were then plated onto polystyrene culture dishes coated with poly-L-lysine and stored in a humidified atmosphere containing 5% CO_2 in air at 37 °C. Neurones were used < 8 h after plating.

Whole-cell voltage clamp recordings

The method for voltage clamping single neurones using the whole-cell variant of the patch-clamp technique (Hamill, Marty, Neher, Sakmann & Sigworth, 1981) has been described previously (Ikeda & Schofield, 1987; Ikeda, 1991). Patch electrodes were made from a borosilicate glass capillary (1·65 mm outer diameter, 1·2 mm inner diameter, Corning 7052, Garner Glass Co., Claremont, CA, USA) using a P-87 Flaming–Brown micropipette puller (Sutter Instrument Co., San Rafael, CA, USA). Pipettes were coated with Sylgard® 184 (Dow Corning, Midland, MI, USA), fire-polished on a microforge (Narishige Scientific Instrument Lab., Tokyo, Japan) and had resistances of 0·5–2 MΩ when filled with the solutions described below. Cell culture dishes were placed on the stage of an inverted microscope and superfused with external solution by gravity at a rate of approximately 2 ml/min. After a gigaohm seal was formed between the pipette and the cell membrane, the patch was ruptured by steady suction. The cell membrane capacitance and series resistance were electronically compensated (typically greater than 80%) using the Axopatch-1C patch-clamp amplifier (Axon Instruments, Foster City, CA, USA). Voltage protocols were generated by a Macintosh IIci computer (Apple Computer, Cupertino, CA, USA) using custom software (Ikeda, 1991, 1992). Traces were digitized at 5 kHz and filtered at 5 kHz using a 4-pole Bessel filter in the clamp amplifier. All experiments were performed at room temperature (21–24 °C). Current traces were normally stored on the hard drive of the computer and later analysed with Igor software (WaveMetrics, Lake Oswego, OR, USA).

Data analysis

Current traces and current–voltage (*I–V*) relationships were corrected for linear leakage current as determined from hyperpolarizing pulses. Tail current amplitudes were measured isochronally 1·5 ms after termination of step pulses (this reduced contribution from Ca^{2+} tail current). Amplitudes of step currents were determined isochronally either 10 ms after the onset or at the termination of a test pulse as indicated below. Least-squares non-linear regression estimates of Boltzmann and exponential functions were performed with Igor curve-fitting functions. Data from different cells were usually normalized as arbitrary units or divided by their membrane capacitances (pA/pF). Data are expressed as means ± standard error of the means (S.E.M.) where appropriate. Student's unpaired *t* test was applied to determine the statistical significance. The differences were considered significant if $P < 0·05$.

Solutions

Hanks' balanced salt solution was made from the powder manufactured by Gibco. $NaHCO_3$ (5 mM) was added to the solution (pH 7·4). Earle's balanced salt solution was made from concentrated liquid (Sigma Chemical Co.) with 10 mM *N*-2-hydroxyethylpiperazine-*N'*-2-ethanesulphonic acid (Hepes), 20 mM glucose and 2·6 mM $NaHCO_3$ (pH 7·4).

For recording Ca^{2+} currents, the pipette solution (denoted 'TEA–NMG internal' solution) contained (mM): 140 NMG–methanesulphonate ($MeSO_3$), 20 TEA–$MeSO_3$, 20 HCl, 11 ethyleneglycol-bis-(β-aminoethyl ether) *N,N,N',N'*-tetraacetic acid (EGTA), 1 $CaCl_2$, 10 Hepes, 4 MgATP (adenosine-5'-triphosphate), 0·1 Na_2GTP (guanosine-5'-triphosphate). The final pH of the solution was adjusted to 7·2 with methanesulphonic acid. The osmolality, as determined with a vapour pressure osmometer, was 305 mosmol kg^{-1}. The external solution (denoted as 'TEA–Ca^{2+} external' solution) consisted of: 145 TEA–$MeSO_3$, 10 Hepes, 10 $CaCl_2$, 15 glucose, 0·0005 TTX, pH 7·4 and 325 mosmol kg^{-1}. KCl was omitted from the external solution since external K^+, under these conditions, produces a transient inward current apparently resulting from K^+ movement

through A-type K^+ channels (Bossu, Dupont & Feltz, 1985; and authors' unpublished data). In external solutions where TEA was replaced, Na^+ was used as a major cation in the external solution ('Na^+–Ca^{2+} external' solution).

In later experiments, the slow tail current was primarily examined in a Ca^{2+}-free external solution ('Na^+ external' solution) and a pipette solution containing mainly NMG–$MeSO_3$ ('NMG internal' solution). The other solutions were only slight modifications of these two basic solutions. The 'Na^+ external' solution contained (mM): 145 NaCl (or $NaMeSO_3$ if specified), 10 $MgCl_2$, 10 Hepes, 15 glucose, 0·0005 TTX, pH 7·4 and 315 mosmol kg^{-1}. In one case, external Na^+ concentration was lowered to 40 mM ('40 Na^+ external') and the osmolality was held constant by adding an appropriate amount of NMG. In some experiments where 145 mM of various monovalent cations (e.g. Rb^+, K^+, Cs^+, and Li^+) was substituted for an equal amount of Na^+, the external solution was named after each cation. The 'NMG internal' solution contained: 150 NMG–$MeSO_3$, 20 HCl, 11 EGTA, 10 Hepes, pH 7·2 and 305 mosmol kg^{-1}. In experiments where the reversal potentials were examined, 40 mM Na^+ was substituted for an equal amount of NMG ('40 Na^+ internal'). In studies where the effect of internal Cs^+ or internal K^+ on the slow tail current was examined, an equimolar amount of NMG was replaced by either 145 mM Cs^+ ('Cs^+ internal') or 12 mM K^+ ('K^+ internal').

RESULTS

Slow inward tail current component in Ca^{2+} current isolation solutions

The top panel of Fig. 1*A* depicts representative Ca^{2+} current traces evoked by 70 ms depolarizing pulses from a holding potential of −80 mV to various test potentials (−20 to +5 mV shown in the figure). The currents were recorded in solutions designed to isolate Ca^{2+} currents in which TEA was the major monovalent cation, Ca^{2+} was the major divalent cation in the external solution ('TEA–Ca^{2+} external'), and NMG–$MeSO_3$ was the major component of the internal solution ('TEA–NMG internal'). Under these conditions, the currents generated during the depolarizing steps were non-inactivating and followed by tail currents that decayed rapidly in agreement with previous studies of Ca^{2+} current in sympathetic neurones (Plummer, Logothetis & Hess, 1989; Jones & Jacobs, 1990; Ikeda, 1991). Conversely, when Na^+ was substituted for TEA in the external solution ('Na^+–Ca^{2+} external'), a prominent slow tail current component was evident following repolarization to −80 mV (bottom traces of Fig. 1*A*). *I–V* relationships for the step current from the same neurone bathed in either 'TEA–Ca^{2+} external' (●) or 'Na^+–Ca^{2+} external' (○) solutions are shown in Fig. 1*B*. In the presence of external Na^+, the amplitude of the step current (measured isochronally 10 ms after depolarization) was increased at potentials between −20 and +20 mV. Tail current amplitudes determined isochronally 1·5 ms after repolarization in either 'TEA–Ca^{2+} external' (●) or 'Na^+–Ca^{2+} external' (○) solutions are illustrated in Fig. 1*C*. When determined at this time delay, tail current amplitudes in the presence of external TEA were negligible compared to those observed in the 'Na^+–Ca^{2+} external' solution. The *I–V* relationship for the slow tail current component was sigmoidal with half-activation occurring near −10 mV. As slow deactivation kinetics are uncharacteristic of high-threshold Ca^{2+} channels (Swandulla & Armstrong, 1988), the ionic basis of the tail current was further investigated.

Ionic basis of the slow inward tail current component

Since 10 mM external Ca^{2+} was present in the above experiments, we tested whether Ca^{2+} and/or voltage-activated Ca^{2+} channels contributed to the slow tail current component. Figure 2*A* shows superimposed current traces from the same

neurone bathed first in the 'Na^+–Ca^{2+} external' solution (with the 'TEA–NMG internal' solution) and then in a solution in which Ca^{2+} was replaced by Mg^{2+} ('Na^+ external'). Although the step current was greatly reduced when Ca^{2+} was removed, as anticipated, the slow tail current component actually slightly increased in

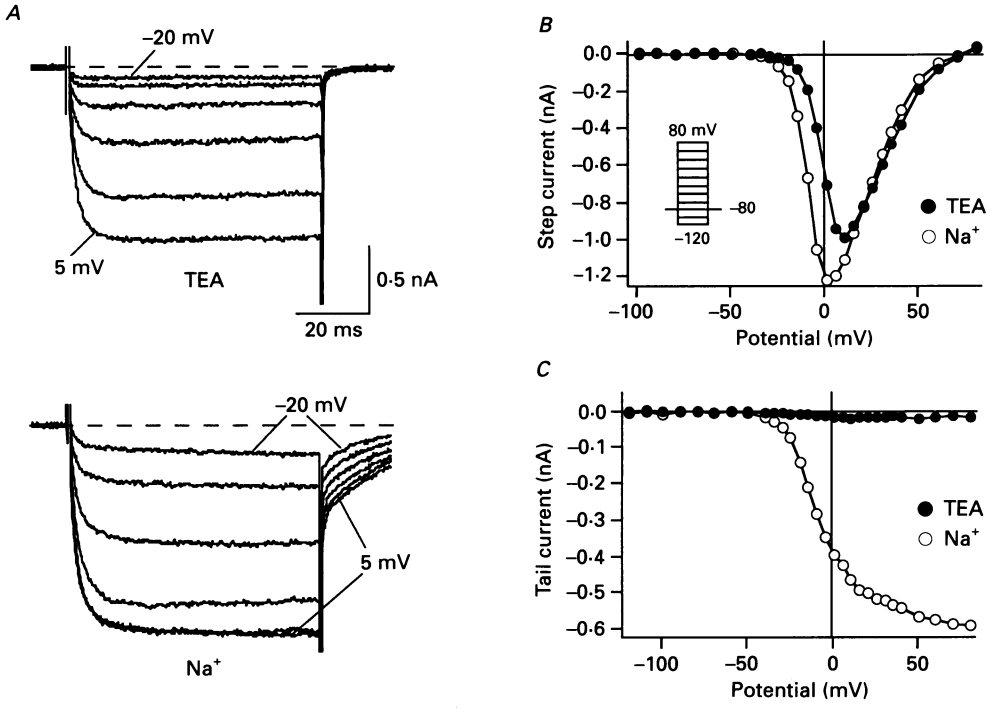

Fig. 1. Na^+-induced slow tail current in SCG neurones. *A*, leak-subtracted step and tail current traces elicited in solutions containing 10 mM Ca^{2+} by 70 ms depolarizing steps from a holding potential of −80 mV to the test potentials indicated by the attached numerals (5 mV increments). The pipette solution consisted primarily of NMG–$MeSO_3$ ('TEA–NMG internal'). Top, TEA was the major external monovalent cation ('TEA–Ca^{2+} external'). Bottom, Na^+ was used to replace TEA ('Na^+–Ca^{2+} external'). Note the presence of the prolonged tail currents. *B*, current–voltage relationship (*I–V* curve) for the step currents in the presence of external TEA (●) or Na^+ (○). The amplitude of the step current was determined isochronally 10 ms after onset of the test pulse (see inset for protocol). *C*, plot of tail current amplitudes *versus* the test potentials in the presence of external TEA (●) or Na^+ (○). The tail current amplitude was determined isochronally 1·5 ms after return to −80 mV. Current traces and the *I–V* curves for the step and the tail currents were from the same neurone.

amplitude under these conditions (○). *I–V* relationships for tail current amplitudes *versus* the step pulse voltage (see inset) are shown in Fig. 2*B*. Tail current amplitudes were similar or slightly larger when Mg^{2+} was substituted for Ca^{2+} in the external solution. We also sought to determine whether the slow tail current component resulted from ions traversing voltage-gated Ca^{2+} channels. To this end, the Ca^{2+} channel-blocking ion Cd^{2+} (0·1 mM) was added to the Na^+–Ca^{2+} external solution. The data represented in Fig. 2*C* demonstrate that Cd^{2+} blocked the majority of the

step current but had virtually no effect on the slow tail current component. Tail current I–V relationships in either the presence (□) or absence (■) of 0·1 mM Cd^{2+} are shown in Fig. 2*D*. The presence of 0·1 mM external Cd^{2+} had no significant effect on tail current amplitude at any voltage studied. Taken together, the results of these

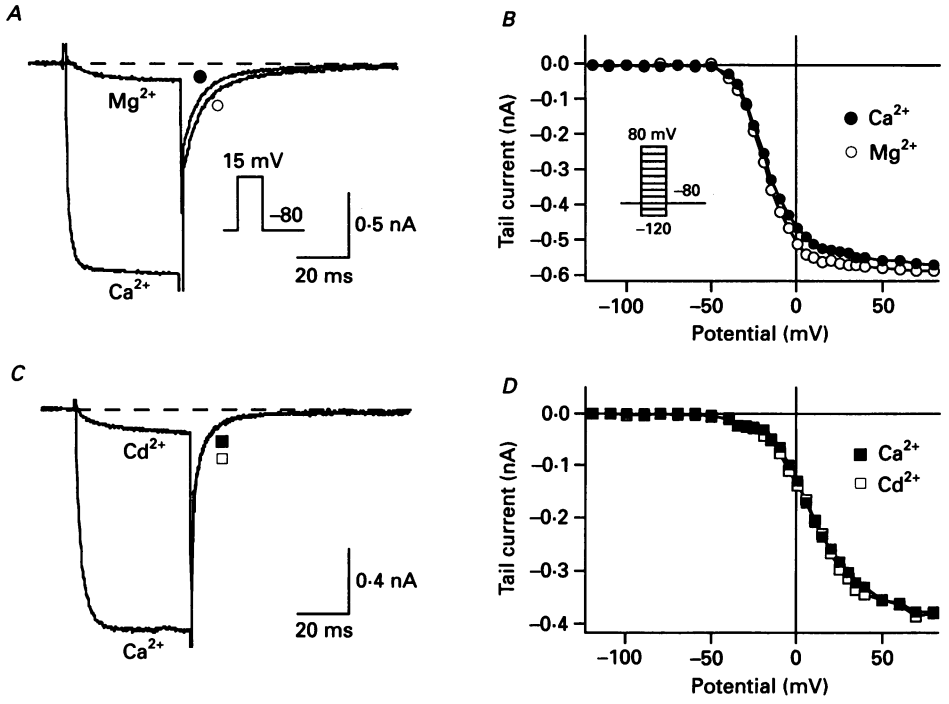

Fig. 2. Removal of external Ca^{2+} or addition of Cd^{2+} had little effect on the slow tail current. *A*, superimposed current traces, generated with the protocol shown, recorded from the same neurone in solutions containing 145 mM Na^+ and either 10 mM Ca^{2+} (●; 'Na^+–Ca^{2+} external') or 10 mM Mg^{2+} (○, 'Na^+ external'). The pipette solution consisted primarily of NMG–$MeSO_3$ ('TEA–NMG internal'). *B*, plot of tail current amplitudes *versus* step potentials (see inset) obtained in the presence of 145 mM Na^+ and 10 mM Ca^{2+} (●) or Mg^{2+} (○). The tail current amplitude was determined isochronally 1·5 ms after return to −80 mV. Data were from the same neurone as in *A*. *C*, superimposed current traces recorded (same protocol as shown in *A*) in the absence (■) or presence (□) of 0·1 mM external Cd^{2+}, a Ca^{2+} channel blocker, in the 'Na^+–Ca^{2+} external' solution. The pipette contained the 'TEA–NMG internal' solution. *D*, I–V curve for the tail currents (data from the same neurone as in *C*) in the absence or presence of 0·1 mM Cd^{2+}. The tail current amplitude was determined as in *B*.

experiments demonstrate that the slow tail current component was (1) not carried by Ca^{2+}, (2) not Ca^{2+} dependent, and (3) not the result of ions flowing through high-threshold voltage-gated Ca^{2+} channels. Therefore, in the following studies, external Ca^{2+} was replaced with Mg^{2+} to eliminate the Ca^{2+} current component while still maintaining charge screening and cell membrane stability. Unless otherwise indicated, the 'Na^+ external' and 'NMG internal' solutions were used in the following studies.

A Cl^- conductance producing prolonged tail currents has been reported in several neuronal and non-neuronal preparations (Mayer, 1985; Evans & Marty, 1986; Owen, Segal & Barker, 1986). As Cl^- was present in both the internal and external solutions in the above experiments, we addressed whether Cl^- might contribute to the slow tail

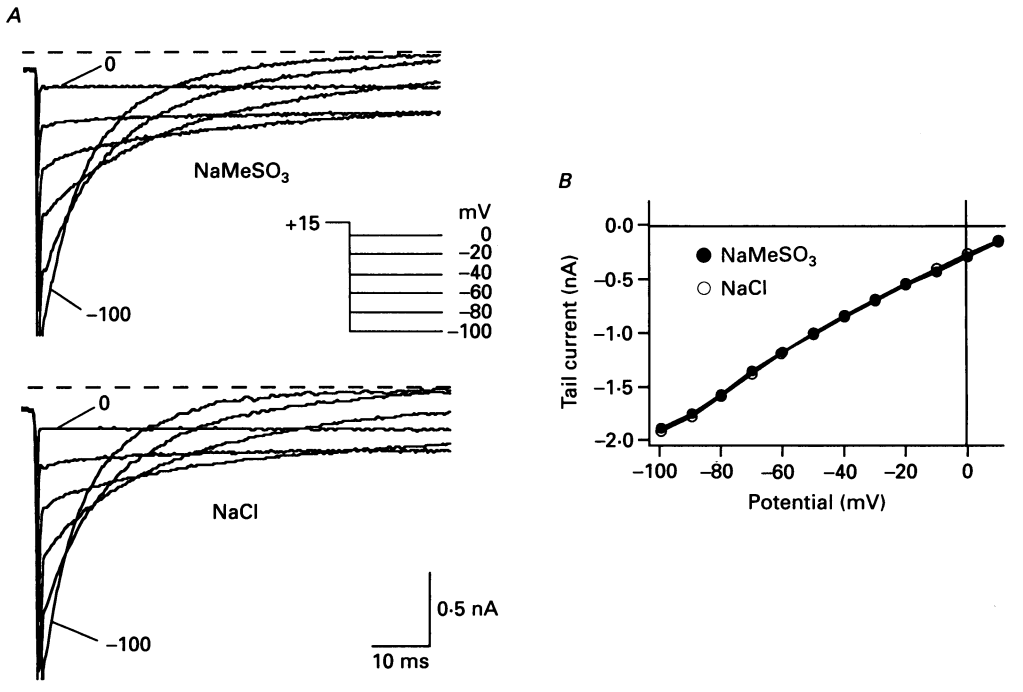

Fig. 3. Chloride does not contribute to the slow tail current. *A*, superimposed tail currents generated upon repolarization to various potentials (inset) from a 50 ms depolarizing pulse to +15 mV. The top traces were obtained in an external solution containing 10 mM $MgCl_2$ and 145 mM $NaMeSO_3$ (20 mM Cl^- total). The bottom traces were obtained after superfusion of the same neurone with external solution containing 10 mM $MgCl_2$ and 145 mM NaCl (165 mM Cl^- total). The internal solution contained 20 mM Cl^- ('NMG internal'). *B*, *I–V* curves for the tail currents in the presence of external $NaMeSO_3$ (●) or NaCl (○). The amplitude of the tail current was measured isochronally 1·5 ms after returning to various test potentials from the same neurone as shown in *A*.

current component. To this purpose, we examined tail currents recorded in external solutions containing 145 mM of either $NaMeSO_3$ or NaCl ('Na^+ external'). Superimposed tail current traces obtained in the 'Na^+ external' (where $NaMeSO_3$ was used) and in the 'NMG internal' solution (both containing 20 mM Cl^-) are shown in Fig. 3*A* (top). Tail currents were determined at different potentials following a constant step potential to +15 mV (Fig. 3*A*, inset). In the presence of equal internal and external [Cl^-], the predicted reversal potential for a Cl^- current is 0 mV. However, substantial inward current remained at 0 mV under these conditions and the extrapolated reversal potential was clearly greater than 0 mV (Fig. 3*B*, ●). Furthermore, substitution of NaCl for $NaMeSO_3$ in the external solution produced no significant changes in either the tail current trajectory (Fig. 3*A*, bottom traces) or

extrapolated reversal potential (Fig. 3*B*, ○). Under these conditions, the predicted reversal potential for Cl^- was −53 mV. These data suggest that Cl^- does not significantly contribute to the slow inward tail current component.

As Ca^{2+} and Cl^- did not appear to contribute significantly to the tail current, the most likely charge carrier was Na^+. We first examined the effect of substitution of

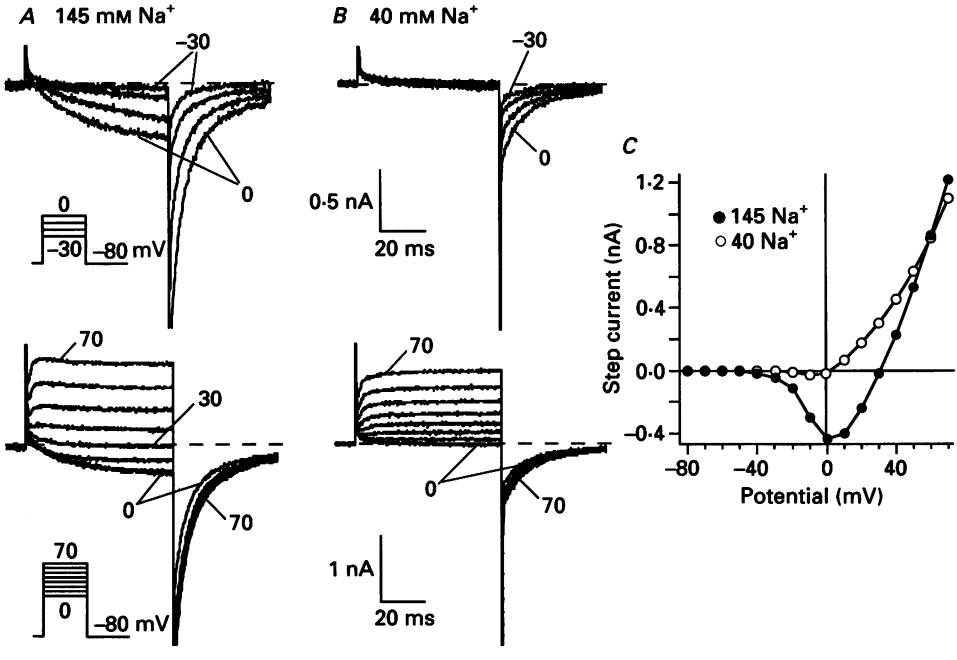

Fig. 4. Dependence of step current reversal potential on $[Na^+]_o/[Na^+]_i$. *A*, superimposed current traces evoked with 70 ms pulses to the test potentials indicated (10 mV increment) in solutions containing 145 mM external Na^+ ('Na^+ external') and 40 mM internal Na^+ ('40 Na^+ internal'). The attached numerals indicate the step potential from which either the step current or the tail current was generated. *B*, superimposed current traces, recorded from the same neurone with the identical protocol as in *A*, following superfusion with external solution containing 40 mM Na^+ ('40 Na^+ external'). *C*, *I–V* curves of the step current amplitude (measured isochronally 65 ms after the onset of the test pulse) *versus* the step potential in either 145 mM (●) or 40 mM external Na^+ (○). Data are from the same neurone shown in *A* and *B*.

Na^+ with other non-permeant ions on the tail currents. We found that the tail current was completely abolished in the external solution in which Na^+ was replaced by tris(hydroxymethyl)-aminomethane (Tris) or NaCl was replaced by sucrose (data not shown). These results, however, did not rule out the possibility that a Na^+-activated event contributed to the slow tail current. To address this question, we determined the reversal potentials of both the step and tail currents in the presence of various concentrations of external Na^+. Figure 4*A* illustrates current traces produced in solutions containing 145 mM of external Na^+ ('Na^+ external') and 40 mM of internal Na^+ ('40 Na^+ internal'). Under these conditions, step depolarizations between −30 and +30 mV resulted in slowly activating inward currents followed by large inward tail currents. At step potentials positive to +30 mV, step currents were

outward and did not significantly inactivate during the 70 ms pulse. Following superfusion with external solution containing 40 mM Na^+ ('40 Na^+ external'), inward step currents were negligible and outward currents occurred at potentials positive to 0 mV (Fig. 4*B*). *I–V* relationships for the step currents illustrated in Fig. 4*A* and *B*

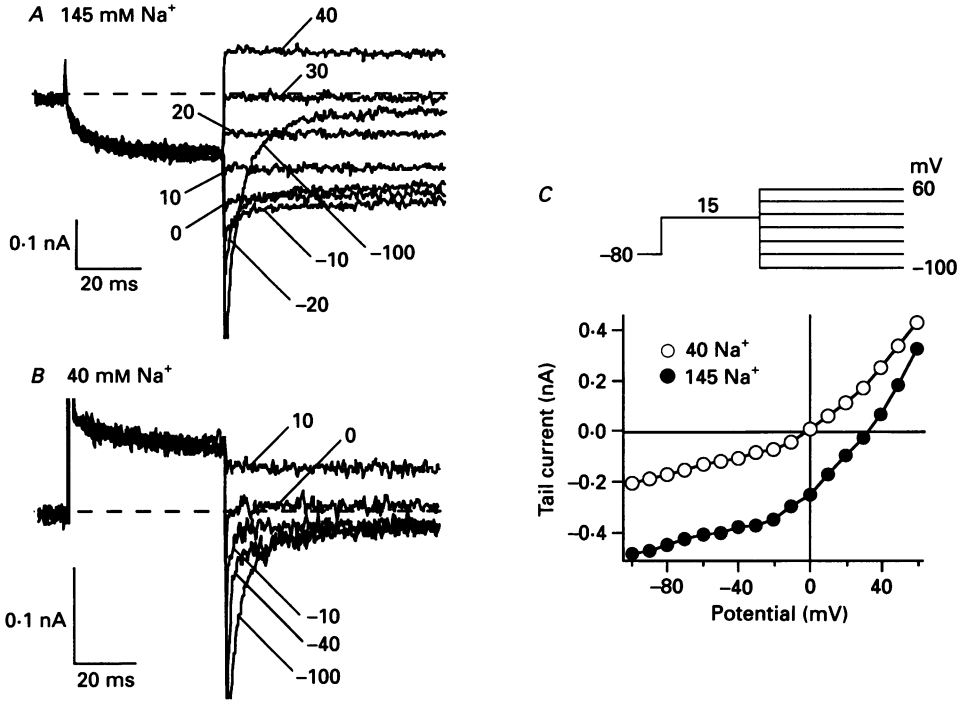

Fig. 5. Dependence of tail current reversal potential on $[Na^+]_o/[Na^+]_i$. *A*, superimposed current traces recorded in the presence of 145 mM external Na^+ and 40 mM internal Na^+ (same solutions as in Fig. 4*A*). Tail currents were generated at different potentials (attached numerals, mV) following a constant step to +15 mV (see protocol in *C*). For clarity, only selected traces are shown. *B*, superimposed current traces, recorded from the same neurone with the identical protocol as in *A*, following superfusion with external solution containing 40 mM Na^+ ('40 Na^+ external'). *C*, *I–V* relationship of the tail current amplitude *versus* the returning potential in the presence of 145 mM (●) or 40 mM (○) external Na^+. Data are from the same neurone shown in *A* and *B*.

are shown in Fig. 4*C*. Reducing external Na^+ concentration from 145 to 40 mM shifted the reversal potentials from about +32 mV (●, +31 ± 2·5 mV, $n = 9$) to near 0 mV (○, +0·8 ± 1·3 mV, $n = 4$). This shift is consistent with that predicted by the Nernst equation for a Na^+ electrode, suggesting that Na^+ is the major charge carrier for the step currents under these conditions.

Figure 5*A* and *B* show selected tail current traces observed in the 'Na^+ external' and the '40 Na^+ external' solutions, respectively, from the same neurone. The pipette was filled with the '40 Na^+ internal' solution. Tail currents were recorded at various potentials following a 50 ms step to 15 mV (see Fig. 5*C* for protocol). The *I–V* relationship of the tail current amplitudes shown in Fig. 5*A* and *B* is illustrated in Fig. 5*C*. Changing the external Na^+ from 145 to 40 mM shifted the reversal potential

of the tail current from about +30 mV (●) to near 0 mV (○). These data are consistent with the step current reversal potential measurements. Taken together, the results of experiments shown in Figs 4 and 5 establish Na^+ as the major charge carrier for both the step current and the prolonged tail current in these solutions. In

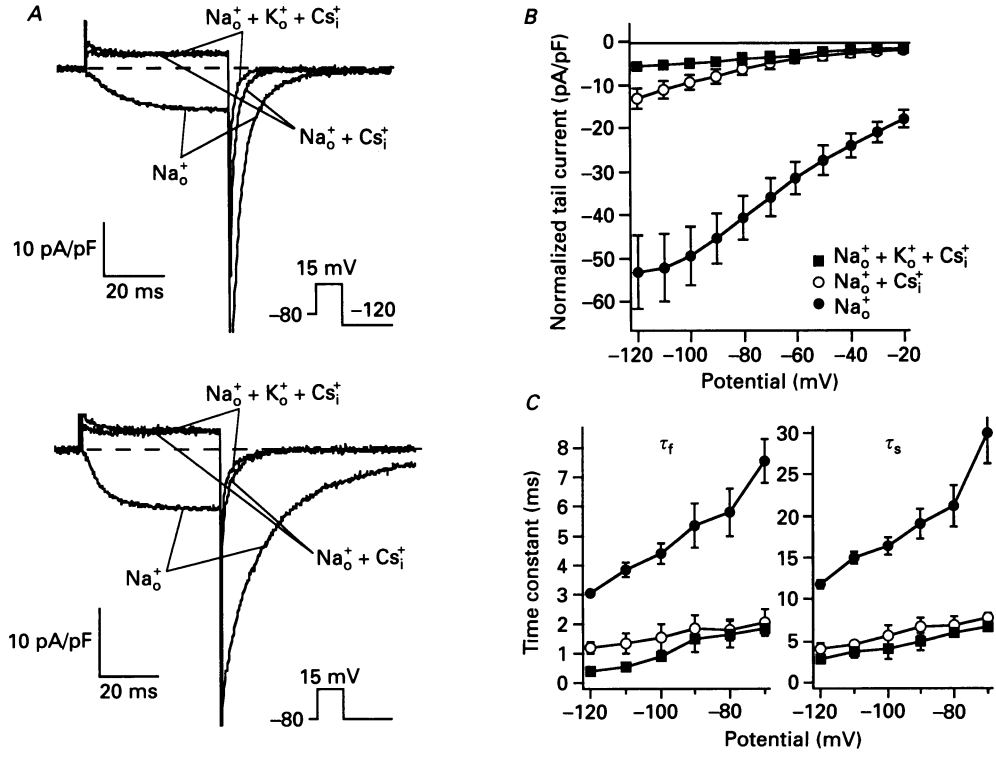

Fig. 6. The slow inward tail current is reduced by internal Cs^+ and external K^+. *A*, superimposed current traces were elicited with the protocols shown (insets) and normalized to membrane capacitance. Traces were recorded from different neurones bathed in the following solutions: (1) Na_o^+: 145 mM external Na^+ and 150 mM internal NMG; (2) $Na_o^+ + Cs_i^+$: 145 mM external Na^+ and 145 mM internal Cs^+; and (3) $Na_o^+ + K_o^+ + Cs_i^+$: 145 mM external Na^+ plus 5·4 mM K^+ and 145 mM internal Cs^+. External TEA (20 mM) was present in (2) and (3). *B*, mean normalized tail current amplitudes recorded under three different conditions (as in *A*) are plotted against the returning potentials (see Fig. 5*C* for protocol). Data were collected from three to five cells. *C*, mean time constants of the tail currents recorded under three different conditions (using the same symbols as in *B*). Decay of the tail currents was fitted to a two-exponential function with non-linear least-squares regression analysis. Left panel, fast component of the time constant; right panel, slow component of the time constant.

the presence of a high concentration of divalent cation (e.g. 10 mM Mg^{2+} in the 'Na^+ external' solution), permeation of Na^+ through voltage-gated Ca^{2+} channels is very unlikely to occur (Almers & McCleskey, 1984). Meanwhile the permeability of the Ca^{2+} channel to Mg^{2+} is negligible (peak step current was < 80 pA in an external solution containing 10 mM Mg^{2+} and 145 mM Tris or sucrose, data not shown; also see Hille, 1992). Therefore, both the step and tail currents appeared to be generated by

the same mechanism in the 'Na^+ external' solution. Cd^{2+} (0·1 mM, added to the 'Na^+ external' solution) had little effect on either the step or the tail current confirming this notion (data not shown). As we have isolated the current carried by Na^+ under our experimental conditions, for convenience, hereafter, this current is referred to as I_u (unusual or unanticipated current).

I_u was reduced by internal Cs^+ and external K^+

As previous whole-cell patch-clamp studies of Ca^{2+} currents in SCG neurones have utilized Na^+ as the primary cation in the external solution (Wanke, Ferroni, Malgaroli, Ambrosini, Pozzan & Meldolesi, 1987; Beech, Bernheim & Hille, 1992), we thought it peculiar that this prominent tail current component had not been previously observed. One of the main differences in the experimental conditions used in the present study and those used by previous investigators was the inclusion of 5·4 mM K^+ in the external solution and the use of Cs^+ rather than NMG in the pipette solution by others. We thus attempted to mimic the composition of solutions used by other investigators with an external solution containing (mM): 145 Na^+, 5·4 K^+, 20 TEA, 10 Mg^{2+} (instead of Ca^{2+}) and an internal solution containing 145 Cs^+ ('Cs^+ internal'). Superimposed current traces, normalized to membrane capacitance, are shown in Fig. 6*A*. Tail currents in the top and bottom traces were generated upon repolarization to −120 and −80 mV, respectively, following a test pulse to +15 mV (protocol inset). When compared with currents recorded in 'Na^+ external' and 'NMG internal' solutions (Na_o^+), the step currents became outward and the tail currents were attenuated in the presence of internal Cs^+ and external K^+ and TEA (denoted $Na_o^+ + K_o^+ + Cs_i^+$ in the figure). The outward step current was possibly due to the movement of Cs^+ through a TEA-insensitive K^+ or Ca^{2+} channel. Figure 6*B* summarizes the amplitudes of the tail currents normalized with respect to membrane capacitance (i.e. current density). The mean tail current density, recorded at −120 mV in the presence of internal Cs^+ and external K^+ and TEA, was 5·6 ± 1·1 pA/pF (■, $n = 4$) which is about one-tenth of that observed in 'Na^+ external' and 'NMG internal' solutions (●, $n = 5$). The tail current decay was adequately described with two time constants. In the presence of internal Cs^+ and external K^+ and TEA, the fast component (τ_f) ranged from 0·6 to 1·1 ms and the slow component (τ_s) from 2·5 to 7·3 ms between repolarizing potentials of −120 and −70 mV (■, Fig. 6*C*) – about 5 times faster than those observed in the 'Na^+ external' and the 'NMG internal' solutions (●). The attenuation in the I_u tail amplitude appeared to be a result of blockade by internal Cs^+, external K^+ and/or TEA. To understand the blocking mechanism better, we examined the effect of 5·4 mM external K^+ on the slow inward tail current. With pipette solutions containing Cs^+, the amplitude of the tail current was larger in the absence of external K^+ (Fig. 6*A* and *B*, $Na_o^+ + Cs_i^+$ and ○, respectively) and the time constants of the tail current decay were slightly greater (○, Fig. 6*C*). This result suggests that the tail current was partially blocked by external K^+ (see below).

The amplitude of the tail current observed in the presence of internal Cs^+ and external K^+ and TEA was in the range of 100–200 pA (the mean capacitance for single neurones was about 31·5 ± 2·4 pF, $n = 32$ in our studies). This tail current is relatively small compared with the tail current generated in 10 mM external Ca^{2+} (in

the range of 1–3 nA) as previously described (Ikeda, 1991, 1992). Therefore, the large Ca^{2+} tail current could mask the component generated by external Na^+ in the presence of external K^+ and internal Cs^+. However, the decay of the tail current was relatively slow (> 0·6 ms) when compared to the Ca^{2+} tail current (about 0·3 ms;

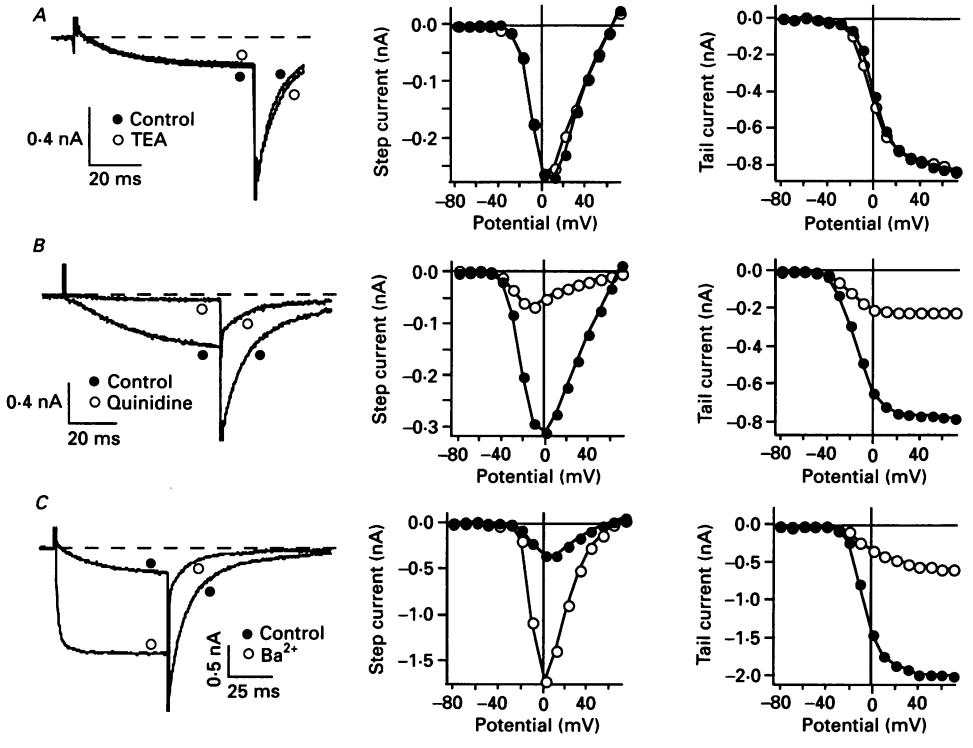

Fig. 7. Effects of K^+ channel blockers on I_u. *A*, left panel, superimposed current traces generated from the same neurone by 70 ms pulse to 0 mV from a holding potential of −80 mV in the absence (●) and presence (○) of 20 mM external TEA. In this and subsequent experiments in this figure, the indicated agent was added directly to the 'Na^+ external' solution and the pipette contained the 'NMG internal' solution. Sucrose was added to the 'Na^+ external' solution when necessary to maintain osmolality constant with the drug-containing solution. Middle panel, *I–V* curve for step current in the absence (●) and presence (○) of 20 mM external TEA. Currents were generated with the protocol shown in Fig. 1*B* and measured at the termination of the step pulse. Right panel, *I–V* curves of the tail currents recorded in external solutions with (○) or without (●) TEA. Tail current amplitude was determined 1·5 ms following the termination of the step pulse. Data presented in *A* were from the same neurone. *B*, superimposed current traces (left panel), *I–V* curves of the step current (middle panel) and the *I–V* curves of tail current (right panel) in the absence (●) and presence (○) of 0·1 mM external quinidine. Protocols were similar to those used in *A*. *C*, superimposed current traces (left panel), *I–V* curves of the step current (middle panel) and the *I–V* curves of tail current (right panel) in the absence (●) and presence (○) of 5 mM external Ba^{2+}. Protocols were similar to those used in *A*.

Ikeda, 1991). Thus, the slow tail current may significantly contaminate Ca^{2+} tail current measurements under these conditions, especially at more delayed time points.

Pharmacology of I_u

As described in Fig. 6, I_u tail amplitude was reduced by a combination of internal Cs^+ and external K^+ and TEA. We examined further the effect of external TEA on I_u from SCG neurones. Superimposed current traces, evoked by a 70 ms step to +10 mV from a holding potential of −80 mV in the absence (●) and presence (○) of 20 mM TEA in the Na^+ external solution, are shown in the left panel of Fig. 7*A*. Under these conditions, TEA had no apparent effect on the step and tail currents (about 30 mM sucrose was added to the TEA-free solution to keep the osmolality at the same level as that of the TEA-containing solution: 335 mosmol kg^{-1}). *I–V* relationships for step currents recorded in the absence (●) or presence of TEA (○) are shown in the middle panel of Fig. 7*A*. Current amplitudes were similar at all potentials in the presence or absence of TEA (data representative of five neurones). A small outward current, which occurred at very positive potentials (e.g. +70 mV in this case), appeared to be due to residual internal K^+ since its amplitude decreased with time. The right panel of Fig. 7*A* illustrates the *I–V* relationship of the tail current determined in the absence (●) or presence of TEA (○). TEA had minimal effect on the tail current amplitude, indicating that the block seen in Fig. 6 was primarily produced by the internal Cs^+ and the external K^+. Taken together, the data presented in Figs 6 and 7*A* led us to hypothesize that I_u might arise from Na^+ passing through TEA-insensitive voltage-gated K^+ channels. Therefore, we further studied several K^+ channel blockers on I_u. Figure 7*B* shows that 0·1 mM quinidine (added to 'Na^+ external') blocked both the step (middle panel) and the tail current (right panel) by about 75·3 ± 6·4% ($n = 5$). Quinidine at 1 mM was able to block I_u almost completely (data not shown). Barium at 5 mM (added to 'Na^+ external') also blocked the tail current amplitude by about 77 ± 6·5% (left and right panel of Fig. 7*C*, $n = 3$) although the step current was increased, presumably due to Ba^{2+} flowing through voltage-gated Ca^{2+} channels (middle panel of Fig. 7*C*). Dendrotoxin at 10 μM had no effect on I_u (data not shown). The fact that I_u is sensitive to K^+ channel blockers such as Ba^{2+} and quinidine further indicates a similarity between the I_u-generating channel and a K^+ channel. Therefore, we compared the currents generated in external Na^+ with those in external K^+.

Comparison of I_u with TEA-insensitive K^+ currents

Representative current traces, elicited in the presence of 145 mM external Na^+ ('Na^+ external') or K^+ ('K^+ external') and with the 'NMG internal' solution in the pipette, are shown in Fig. 8*A* and *B*, respectively. TEA (20 mM) was present in both external solutions to isolate the TEA-insensitive K^+ channel. Currents were elicited by 70 ms depolarizing pulses to various step potentials from a holding potential of −80 mV. In the presence of 'Na^+ external', currents were similar to those previously described (see Fig. 4*A*). When currents were recorded in 'K^+ external', a transient inward current appeared at potentials positive to −60 mV which largely inactivated during the 70 ms pulse (Fig. 8*B*). The transient inward current was probably conducted by 'A-type' K^+ channels because (1) the current was abolished at a holding potential of −50 mV (data not shown), (2) the kinetics of the current were similar to those previously described for the 'A-current' in SCG neurones (Schofield & Ikeda,

1989), and (3) the current persisted in the presence of 20 mM TEA. At step potentials positive to −40 mV, a non-inactivating step current component was present which was followed by an inward tail current. This K^+ current was probably flowing through TEA-insensitive delayed rectifier-type channels. The decay of the tail

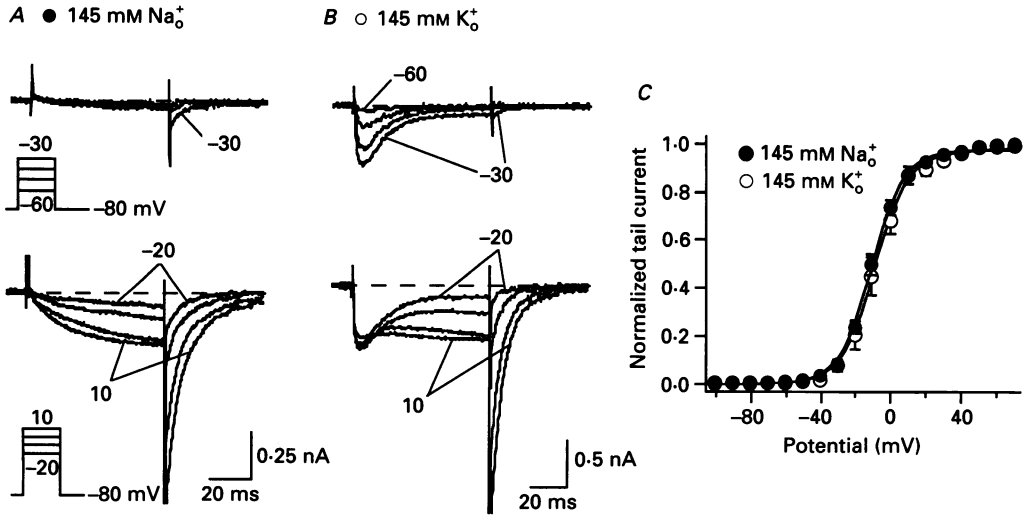

Fig. 8. Similarity between I_u and TEA-insensitive K^+ currents. *A*, superimposed current traces elicited with the protocol shown (insets) in the 'Na^+ external' and 'NMG internal' solutions. TEA (20 mM) was added to the external solution. *B*, superimposed current traces recorded from the same neurone shown in *A* after superfusion with solution in which K^+ was substituted for Na^+ ('K^+ external'). TEA (20 mM) was also present in this solution. *C*, activation curves derived from mean tail current amplitudes ($n = 5$–9) with Na^+ (●) or K^+ (○) as the primary charge carrier. Amplitudes were normalized to the maximal value. Each curve represents the best fit of the data to a modified Boltzmann equation (see text).

current was similar whether recorded in 'Na^+ external' or 'K^+ external'. For example, τ_f was 5·8±0·8 ($n = 9$) and 5·6±0·8 ms ($n = 5$), and τ_s was 21·2±2·5 and 22·4±5·3 ms for tail currents carried by Na^+ and K^+, respectively (measured following a step potential to +10 mV). Steady-state activation curves, recorded in either 'Na^+ external' (●) or 'K^+ external' (○) solution, are shown in Fig. 8*C*. Each point represents the mean tail current amplitude normalized with respect to the maximum. Data were fitted to a modified Boltzmann equation:

$$i(V) = I[1 + \exp((V_{0.5} - V)/k)]^{-1}, \quad (1)$$

where $i(V)$ is the tail current amplitude following test pulse potential V; I, $V_{0.5}$ and k are maximal current amplitude, half-activation voltage and slope factor, respectively. Activation curves were similar regardless of whether Na^+ or K^+ was the charge carrier. $V_{0.5}$ was −9·4±5·6 ($n = 14$) and −8·8±6·2 mV ($n = 5$), and k was 8·4±1·3 and 9·3±1·0 mV, for activation curves generated in 'Na^+ external' and 'K^+ external', respectively.

Inactivation was determined for the inward step currents generated in the 'K^+

external' or the 'Na^+ external' solution. When cells were depolarized from a holding potential of −80 to +10 mV for 2 s, the decay of the inward step current was very slow with time constants of 2·3 and 2·5 s for external K^+ and Na^+, respectively (data not shown). Taken together, these results suggest that the channel which generates I_u has similar properties to those of TEA-insensitive delayed rectifier-type K^+ channels.

Interaction between Na^+ and K^+

Under physiological conditions, K^+ is the major intracellular monovalent cation. In an attempt to investigate the possible physiological contribution of I_u, we examined the effect of internal K^+ on this current. Figure 9*A* displays superimposed current density traces evoked with a single test pulse (see inset) recorded either in the absence ('NMG internal') or presence of 12 mM internal K^+ ('K^+ internal') from two different neurones. The neurones were superfused with 'Na^+ external' solution in both experiments. A low concentration of K^+ was chosen because at high internal [K^+], the outward current was too large to clamp with high fidelity. In the absence of internal K^+, a large inward tail current was observed upon repolarization to −80 mV as described above. In contrast, the inward tail current was markedly reduced in the presence of internal K^+. These data suggest that internal K^+ was able to block the inward tail current generated in 'Na external' solution.

As described in Fig. 6, external K^+ (at 5·4 mM) reduced the tail current observed in external Na^+ even though a large portion of the tail current had already been blocked by internal Cs^+. In the following experiments, we examined the effect of external K^+ on the tail current in the absence of internal Cs^+. Superimposed current traces, evoked with the same voltage protocol as in Fig. 9*A*, in the absence and presence of 5·4 mM external K^+ are depicted in Fig. 9*B*. TEA (20 mM) was added to both external solutions since it reduced current contamination arising from TEA-sensitive K^+ channels and had little effect on I_u (see Fig. 7*A*). Under these conditions, the substantial decrease in the amplitude of I_u (both the step and the tail currents) was considered as a blockade by external K^+.

The block of I_u by external and internal K^+ led us to examine the interaction between external Na^+ and K^+ further. The effect of different concentrations of external K^+ on the tail current amplitude as shown in Fig. 9*B* is summarized in Fig. 9*C*. The amplitude of the tail current was normalized to the tail current amplitude obtained in the presence of 145 mM Na^+ (with no K^+). Alteration in external [K^+] was accomplished by equimolar substitution of Na^+ from the 'Na^+ external' solution – at the extreme, the solution became the 'K^+ external' solution (with 145 mM K^+). TEA, 20 mM, was present in all external solutions. In the presence of 145 mM K^+, the tail current amplitude was approximately twice that in the presence of Na^+ only ([KCl] = 0). However, addition of K^+ to the 'Na^+ external' or Na^+ to the 'K^+ external' solution led to a decrease in the amplitude of the tail current. At between 1 and 10 mM K^+, the tail current amplitude reached a minimum (about 20–25% of the control, $n = 4$–9). A similar phenomenon described as 'anomalous mole-fraction dependence' has been reported for a voltage-gated Ca^{2+} channel (Almers & McCleskey, 1984; Hess & Tsien, 1984), delayed rectifier K^+ channel (Wagoner & Oxford, 1987), inward rectifier K^+ channel (Hagiwara, Miyazaki, Krasne & Ciani,

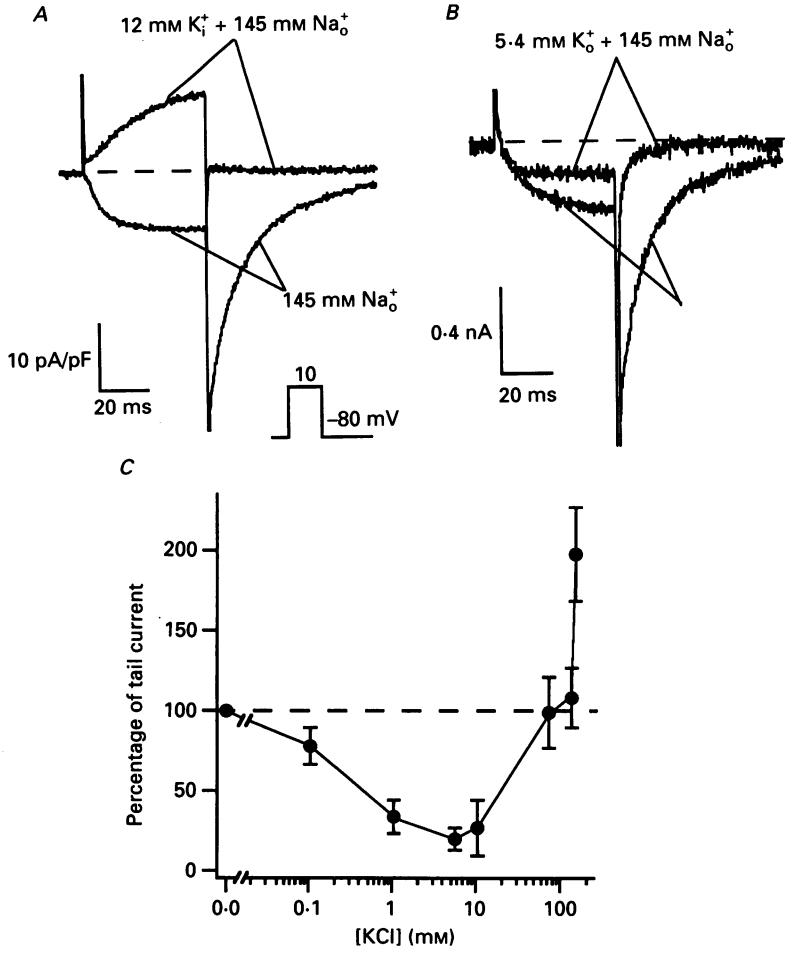

Fig. 9. Effect of external and internal K^+ on I_u. *A*, superimposed current traces observed with a single pulse protocol (see inset) in the absence (145 mM Na_o^+) and presence (12 mM K_i^+ + 145 mM Na_o^+) of 12 mM internal K^+. In the latter condition, 12 mM K^+ was substituted for an equal amount of NMG in the 'NMG internal' solution. Neurones were bathed in 'Na^+ external' with 20 mM TEA. Data were from two different cells and normalized to cell capacitance. *B*, superimposed current traces recorded in the absence (145 mM Na_o^+) and presence (5·4 mM K_o^+ + 145 mM Na_o^+) of 5·4 mM external K^+. In the latter condition, 5·4 mM K^+ was added to the 'Na^+ external' solution. Under both conditions, 20 mM TEA was present in the external solution. Data were from the same neurone. Currents were generated using the same protocol as in *A*. *C*, plot of mean normalized tail current amplitude *versus* external [K^+]. Data were derived under conditions similar to those shown in *B*. For each [K^+], equimolar KCl was substituted for NaCl in the 'Na^+ external' solution (n = 4–9). The amplitude of the tail current was normalized to the one obtained in the absence of external K^+.

1977) and Ca^{2+}-activated K^+ channel (Eisenman, Latorre & Miller, 1986). The interactions between Na^+ and K^+ imply that the channel generating I_u has a multiple-ion pore similar to most known voltage-gated K^+ channels.

Permeability sequence

The relative selectivity of this putative K^+ channel to several monovalent cations was examined using bi-ionic solutions where the internal solution contained 40 mM Na^+ ('40 Na^+ internal') and the external solution contained 10 mM Mg^{2+} and a

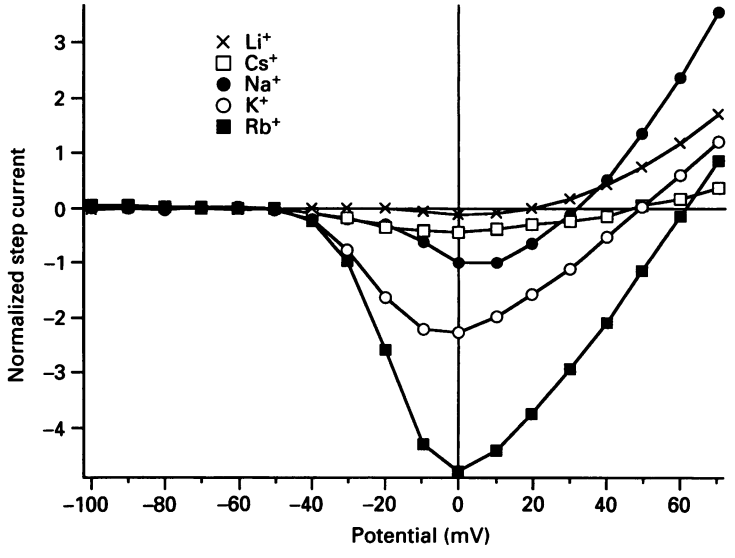

Fig. 10. *I–V* curves of the normalized step current recorded in the presence of 40 mM internal Na^+ and 145 mM external Rb^+, K^+, Cs^+, Na^+ or Li^+. External TEA (20 mM) was present under all conditions. Step currents were generated as in Fig. 1*B* and normalized to maximum inward current obtained in the presence of 145 mM external Na^+. Reversal potentials were estimated from the zero current interception of the *I–V* curve. Data were from different neurones.

145 mM concentration of various cations (Rb^+, K^+, Cs^+, Na^+, and Li^+). TEA at 20 mM was always present in the external solution. Figure 10 shows examples of step current *I–V* relationships in the presence of Rb^+, K^+, Cs^+, Na^+ and Li^+. As the step current and the tail current were generated by the same mechanism under conditions where Ca^{2+} was replaced by Mg^{2+} (Figs 4 and 5), substitution of step current for tail current to determine the relative permeability sequence for five monovalent cations appeared to be valid. The step current amplitudes, determined at the termination of a 70 ms test pulse, were normalized to the maximum inward current obtained in 'Na^+ external' solution. The mean reversal potential for each cation was $57 \pm 3{\cdot}5$ ($n = 3$), $52 \pm 4{\cdot}2$ ($n = 6$), $47 \pm 3{\cdot}3$ ($n = 4$), $31 \pm 2{\cdot}5$ ($n = 9$), and $21 \pm 1{\cdot}4$ mV ($n = 2$) for Rb^+, K^+, Cs^+, Na^+ and Li^+, respectively. Relative permeabilities were determined from changes in the reversal potential (ΔE_{rev}) according to the modified Goldman–Hodgkin–Katz equation:

$$\Delta E_{rev} = E_X - E_{Na} = RT/F(P_X[X]_o/P_{Na}[Na^+]_o), \quad (2)$$

where E_X and E_{Na} are the reversal potentials of the test ion and Na^+, respectively, P_X and P_{Na} are permeabilities of the test ion and Na^+, respectively, $[X]_o$ and $[Na^+]_o$

are the external concentration of test ion and Na^+, respectively. The order of P_X/P_{Na} was as follows: $Rb^+ > K^+ > Cs^+ > Na^+ > Li^+$ with a ratio of 3·5:2·5:2·0:1:0·6. It appears that this channel prefers K^+ to Na^+ although its selectivity over various monovalent cations is relatively poor. However, this sequence of the relative permeability suggests that this channel is more like a K^+ channel than any other known voltage-gated cation channel.

DISCUSSION

In the absence of internal and external K^+, an unanticipated voltage-activated current (I_u) was observed in freshly isolated SCG neurones. I_u was carried primarily by Na^+ as: (1) both the step and tail current reversal potentials shifted as predicted by the Nernst equation; (2) the current was abolished when Na^+ was replaced with Tris or sucrose, and (3) Ca^{2+} and Cl^- did not appear to contribute to I_u as substitution of external Ca^{2+} with Mg^{2+} and external Cl^- with $MeSO_3^-$ did not significantly alter the current, respectively.

The ion channel responsible for this anomalous Na^+ conductance did not appear to be a voltage-gated Na^+ channel for the following reasons. Firstly, the current was observed in the presence of TTX despite the fact that the voltage-activated Na^+ current in SCG neurones is completely blocked by this agent (Schofield & Ikeda, 1988). Secondly, the relative permeability sequence of this channel is not characteristic of a Na^+ channel. Finally, both TTX-sensitive and -insensitive Na^+ channels (found in sensory neurones) inactivate more rapidly than the channel responsible for I_u. In addition, voltage-gated Ca^{2+} channels did not significantly contribute to I_u as the current persisted in the presence of the Ca^{2+} channel blocker, Cd^{2+}. Moreover, although Na^+ may pass through voltage-gated Ca^{2+} channels under circumstances where the divalent cation concentration in external solutions is very low (Almers & McCleskey, 1984; Hess & Tsien, 1984), this is not the case in our experiments since I_u was observed in the presence of 10 mM Ca^{2+} or Mg^{2+}.

We initially discarded the idea that Na^+ was travelling through a K^+ channel as our original internal solution contained the K^+ channel-blocking agent TEA and the permeability of K^+ channels to Na^+ is reported to be very low (Hille, 1992). However, our studies suggest that anomalous permeation of Na^+ through one or more TEA-insensitive K^+ channel(s) may be responsible for I_u. Several lines of experimental evidence support this notion. Firstly, the properties of the channel which generates I_u are similar to those of delayed rectifier-type K^+ channels, i.e. both activate at the same voltage (about -40 to -30 mV) and inactivate very slowly. The time constants of the I_u tail current are also similar to those of delayed rectifier-type K^+ channels. Secondly, the I_u tail current can be blocked by conventional K^+ channel blockers such as quinidine, Ba^{2+} and Cs^+. Although quinidine is not a very selective blocker for K^+ channels – it has been shown to block voltage-gated Na^+ and Ca^{2+} channels (Hermann & Gorman, 1984) – the ability of Ba^{2+} and Cs^+, known blockers for several K^+ channels, to block the slow tail current does suggest a K^+ channel similarity. The lack of sensitivity to TEA does not exclude the participation of a K^+ channel as TEA-resistant K^+ channels are known to exist (Rudy, 1988; Stühmer *et al.* 1989). Thirdly, an anomalous mole-fraction dependence was observed when both Na^+ and K^+ were present, suggesting a channel with multiple occupations similar to

most known K^+ channels (Eisenman *et al.* 1986; Hagiwara *et al.* 1977; Wagoner & Oxford, 1987). The attenuation of Na^+ permeation by both external and internal K^+ lead us to speculate that in the absence of external K^+ (and/or internal K^+), a K^+ channel becomes less selective for Na^+. This idea is consistent with the observation by Armstrong & Miller (1990) that a K^+ channel loses ion selectivity in the absence of external K^+. Furthermore, the ability of external K^+ to modulate the gating of K^+ channels has been shown to be related to TEA sensitivity (Pardo *et al.* 1992). In this last study, external K^+ was very effective in modulating gating for a K^+ channel with low sensitivity to TEA (RCK4). In contrast, external K^+ had little effect on the gating of TEA-sensitive K^+ channels (such as RCK1, RCK2, etc.). The channel which generates I_u does not appear to share a similarity with the A-type K^+ channel because the latter activates much earlier (at about -70 to -60 mV) and inactivates very quickly (Schofield & Ikeda, 1989). Although our experimental evidence points to a TEA-insensitive K^+ channel, we cannot exclude the possibility of a novel non-specific cation channel with similar kinetics to K^+ channels.

Sodium ions traversing the K^+ channel has been described in giant squid axons under extreme conditions when a very positive depolarization (> 160 mV) was applied (French & Wells, 1977). In the present study, the conditions which favour anomalous Na^+ permeation were unique and accidental. Potassium was excluded from the external solution because even at 5 mM, external K^+ will pass the A-type K^+ channel to generate an inward current that is very similar to T-type Ca^{2+} current (Bossu, Dupont & Feltz, 1985; and authors' unpublished observation). Cs^+ was not used as the major cation in the internal solution since Cs^+ permeates through Ca^{2+} channels (Bean, 1989), TEA-sensitive (authors' unpublished observation) and -insensitive K^+ channels (the present study) to generate large outward currents. Very interestingly, both external K^+ and internal Cs^+ significantly block I_u. This may well explain the absence of previous reports of this unusual current in SCG since both internal Cs^+ and external K^+ were used in studies by others. It is noteworthy that in the presence of external K^+ and internal Cs^+, 145 mM external Na^+ still produced a rather small but slow tail current which may contaminate Ca^{2+} tail current measurements. Therefore, it may be prudent to avoid the use of solutions containing external Na^+ and K^+, and internal Cs^+ to study Ca^{2+} tail currents. Instead, Tris may be a good candidate as the major monovalent cation in the external solution.

In summary, our studies suggest that the absence of external K^+ results in anomalous permeation of Na^+ through a TEA-insensitive K^+ channel. For practical reasons, caution should be observed when Ca^{2+} currents are studied in the presence of external Na^+ as unanticipated Na^+ permeation may confound data interpretation.

The authors wish to thank Elizabeth Zboran for excellent technical assistance. This work was supported by NIH grant HL-43242 (S.R.I.), a Grant-in-Aid from the American Heart Association-Georgia Affiliate (S.R.I.), and a Biomedical Research Support grant from the Medical College of Georgia (Y.Z.).

REFERENCES

ALMERS, W. & MCCLESKEY, E. W. (1984). Non-selective conductance in calcium channels of frog muscle: calcium selectivity in a single-file pore. *Journal of Physiology* **353**, 585–608.

ARMSTRONG, C. M. & MILLER, C. (1990). Do voltage-dependent K^+ channels require Ca^{2+}? A critical test employing a heterologous expression system. *Proceedings of the National Academy of Sciences of the USA* **87**, 7579–7582.

BEAN, B. P. (1989). Neurotransmitter inhibition of neuronal calcium current by changes in channel voltage dependence. *Nature* **340**, 153–156.

BEECH, D. J., BERNHEIM, L. & HILLE, B. (1992). Pertussis toxin and voltage dependence distinguish multiple pathways modulating calcium channels of rat sympathetic neurons. *Neuron* **8**, 97–106.

BOSSU, J. L., DUPONT, J. L. & FELTZ, A. (1985). I_A current compared to low threshold calcium current in cranial sensory neurones. *Neuroscience Letters* **62**, 249–254.

BROWN, D. A. & CONSTANTI, A. (1980). Intracellular observations on the effects of muscarinic agonists on rat sympathetic neurones. *British Journal of Pharmacology* **70**, 593–608.

CAULFIELD, M. P. (1991). Muscarinic receptor-mediated inhibition of voltage-activated Ca current in neuroblastoma × glioma hybrid (NG108-15) cells – reduction of muscarinic agonist and antagonist potency by tetraethylammonium (TEA). *Neuroscience Letters* **127**, 165–168.

EISENMAN, G., LATORRE, R. & MILLER, C. (1986). Multi-ion conduction and selectivity in the high-conductance Ca^{++}-activated K^+ channel from skeletal muscle. *Biophysical Journal* **50**, 1025–1034.

EVANS, M. G. & MARTY, A. (1986). Calcium-dependent chloride current in isolated cells from rat lacrimal glands. *Journal of Physiology* **378**, 437–460.

FRENCH, R. J. & WELLS, J. B. (1977). Sodium ions as blocking agents and charge carriers in the potassium channel of the squid giant axon. *Journal of General Physiology* **70**, 707–724.

HAGIWARA, S., MIYAZAKI, S., KRASNE, S. & CIANI, S. (1977). Anomalous permeabilities of the egg cell membrane of a starfish in K^+–Tl^+ mixtures. *Journal of General Physiology* **70**, 269–281.

HAMILL, O. P., MARTY, A., NEHER, E., SAKMANN, B. & SIGWORTH, F. J. (1981). Improved patch-clamp techniques for high-resolution current recording from cells and cell-free membrane patches. *Pflügers Archiv* **391**, 85–100.

HERMANN, A. & GORMAN, A. L. F. (1984). Action of quinidine on ionic currents of molluscan pacemaker neurons. *Journal of General Physiology* **83**, 919–940.

HESS, P. & TSIEN, R. W. (1984). Mechanism of ion permeation through calcium channels. *Nature* **309**, 453–456.

HILLE, B. (1992). *Ionic Channels of Excitable Membranes*. Sinauer Associates Inc., Sunderland, MA, USA.

IKEDA, S. R. (1991). Double-pulse calcium channel current facilitation in adult rat sympathetic neurones. *Journal of Physiology* **439**, 181–214.

IKEDA, S. R. (1992). Prostaglandin modulation of Ca^{2+} channels in rat sympathetic neurones is mediated by guanine nucleotide binding proteins. *Journal of Physiology* **458**, 339–359.

IKEDA, S. R. & SCHOFIELD, G. G. (1987). Tetrodotoxin-resistant sodium current of rat nodose neurones: monovalent cation selectivity and divalent cation block. *Journal of Physiology* **389**, 255–270.

JONES, S. W. & JACOBS, L. S. (1990). Dihydropyridine actions on calcium currents in frog sympathetic neurons. *Journal of Neuroscience* **10**, 2261–2267.

MAYER, M. L. (1985). A calcium-activated chloride current generates the after-depolarization of rat sensory neurones in culture. *Journal of Physiology* **364**, 217–239.

OWEN, D. G., SEGAL, M. & BARKER, J. L. (1986). Voltage-clamp analysis of a Ca^{2+}- and voltage-dependent chloride conductance in cultured mouse spinal neurons. *Journal of Neurophysiology* **55**, 1115–1135.

PARDO, L. A., HEINEMANN, S. H., TERLAU, H., LUDEWIG, U., LORRA, C., PONGS, O. & STÜHMER, W. (1992). Extracellular K^+ specifically modulates a rat brain K^+ channel. *Proceedings of the National Academy of Sciences of the USA* **89**, 2466–2470.

PLUMMER, M. R., LOGOTHETIS, D. E. & HESS, P. (1989). Elementary properties and pharmacological sensitivities of calcium channels in mammalian peripheral neurons. *Neuron* **2**, 1453–1463.

RUDY, B. (1988). Diversity and ubiquity of K channels. *Neuroscience* **25**, 729–749.

SCHOFIELD, G. G. & IKEDA, S. R. (1988). Sodium and calcium currents of acutely isolated adult rat superior cervical ganglion neurons. *Pflügers Archiv* **411**, 481–490.

SCHOFIELD, G. G. & IKEDA, S. R. (1989). Potassium current of acutely isolated adult rat superior cervical ganglion neurons. *Brain Research* **485**, 205–214.

STÜHMER, W., RUPPERSBERG, J. P., SCHRÖTER, K. H., SAKMANN, B., STOCHER, M., GIESE, K. P., PERSCHKE, A., BAUMANN, A. & PONGS, O. (1989). Molecular basis of functional diversity of voltage-gated potassium channels in mammalian brain. *EMBO Journal* **8**, 3235–3244.

SWANDULLA, D. & ARMSTRONG, C. M. (1988). Fast-deactivating calcium channels in chick sensory neurons. *Journal of General Physiology* **92**, 197–218.

WAGONER, P. K. & OXFORD, G. S. (1987). Cation permeation through the voltage-dependent potassium channel in the squid axon. Characteristics and mechanisms. *Journal of General Physiology* **90**, 261–290.

WANKE, E., FERRONI, A., MALGAROLI, A., AMBROSINI, A., POZZAN, T. & MELDOLESI, J. (1987). Activation of a muscarinic receptor selectively inhibits a rapidly inactivated Ca^{2+} current in rat sympathetic neurons. *Proceedings of the National Academy of Sciences of the USA* **84**, 4313–4317.